

PAPER • OPEN ACCESS

# Dynamics of the precessing vortex rope and its interaction with the system at Francis turbines part load operating conditions

To cite this article: A Favrel *et al* 2017 *J. Phys.: Conf. Ser.* **813** 012023

View the [article online](#) for updates and enhancements.

## Related content

- [Hydro-acoustic resonance behavior in presence of a precessing vortex rope: observation of a lock-in phenomenon at part load Francis turbine operation](#)  
A Favrel, C Landry, A Müller *et al.*
- [Numerical simulation of a cavitating draft tube vortex rope in a Francis turbine at part load conditions for different -levels](#)  
J Wack and S Riedelbauch
- [Unsteady hydraulic simulation of the cavitating part load vortex rope in Francis turbines](#)  
J Brammer, C Segoufin, F Duparchy *et al.*

## Recent citations

- [Power Swing Generated in Francis Turbines by Part Load and Overload Instabilities](#)  
David Valentin *et al*



**IOP | ebooks™**

Bringing together innovative digital publishing with leading authors from the global scientific community.

Start exploring the collection—download the first chapter of every title for free.

# Dynamics of the precessing vortex rope and its interaction with the system at Francis turbines part load operating conditions

A Favrel<sup>1</sup>, A Müller<sup>1</sup>, C Landry<sup>1</sup>, J Gomes<sup>1</sup>, K Yamamoto<sup>1</sup> and F Avellan<sup>1</sup>

<sup>1</sup>EPFL Laboratory for Hydraulic Machines, Avenue de Cour 33bis, 1007 Lausanne, Switzerland

E-mail: arthur.favrel@epfl.ch

**Abstract.** At part load conditions, Francis turbines experience the formation of a cavitation vortex rope at the runner outlet whose precession acts as a pressure excitation source for the hydraulic circuit. This can lead to hydro-acoustic resonances characterized by high pressure pulsations, as well as torque and output power fluctuations. This study highlights the influence of the discharge factor on both the vortex parameters and the pressure excitation source by performing Particle Image Velocimetry (PIV) and pressure measurements. Moreover, it is shown that the occurrence of hydro-acoustic resonances in cavitation conditions mainly depend on the swirl degree of the flow independently of the speed factor. Empirical laws linking both natural and precession frequencies with the operating parameters of the machine are, then, derived, enabling the prediction of resonance conditions on the complete part load operating range of the turbine.

## 1. Introduction

Francis turbines operating at off-design conditions experience the development of unfavorable flow patterns inducing cavitation and pressure pulsations, such as inter-blade cavitation vortices for very low values of discharge [1] or a self-oscillating cavitation vortex in the draft tube at full load conditions [2]. At part load conditions, the precessing cavitation vortex rope acts as a pressure excitation source for the hydraulic circuit, leading to the propagation of pressure fluctuations at the precession frequency in the whole system [3]. The presence of cavitation in the vortex core decreases the local wave speed and therefore the system eigenfrequencies [4] leading to the risk of resonance [5].

In the framework of the HYPERBOLE research project, the dynamics behavior of the part load vortex rope has been extensively investigated by model tests. This article reports the main results and observations, which led finally to the establishment of empirical laws enabling the prediction of resonance conditions at the reduced model scale. First, the influence of the discharge factor on the vortex dynamics in cavitation-free conditions is investigated by means of both pressure and Particle Image Velocimetry (PIV) measurements. In a second part, the interaction between the excitation source and the system eigenfrequencies is investigated in cavitation conditions by identifying the resonance conditions for different values of the speed factor, as well as the influence of the discharge factor on the precession and natural frequencies. Dimensionless laws linking both natural and precession frequencies with the operating parameters are, then, established, enabling the prediction of resonance occurrences on the complete part load operating range of the reduced scale model.



## 2. Test-case and experimental set-up

The test-case is a reduced scale physical model of a Francis turbine featuring 16 blades and 20 guide vanes installed on the close-loop test rig of EPFL Laboratory for Hydraulic Machines. The upper part of the hydraulic circuit is given in Figure 1, including the upstream pipe, the spiral casing, the draft tube and the downstream reservoir. Pressure fluctuations are measured on the test-rig by flush-mounted piezo-resistive pressure sensors. Their location is given in Figure 1. Four pressure sensors are installed in one horizontal cross-section of the draft tube cone and regularly spaced by an angle of  $90^\circ$ , enabling the decomposition of the pressure fluctuations into convective and synchronous components. In the upstream pipe, two pressure sensors are installed, enabling the direct measurement of the synchronous pressure fluctuation and therefore the estimation of the system hydro-acoustic response.

PIV measurements are also performed in two different horizontal cross-sections of the draft tube cone by using the same set-up than presented in [6]. The optical access for the camera is provided by a Plexiglass window at the bottom of the draft tube elbow. The acquisition of the PIV images is synchronized with pressure measurements, enabling a phase averaging of the flow velocity fields to recover their periodical evolution over one precession period [6, 7].

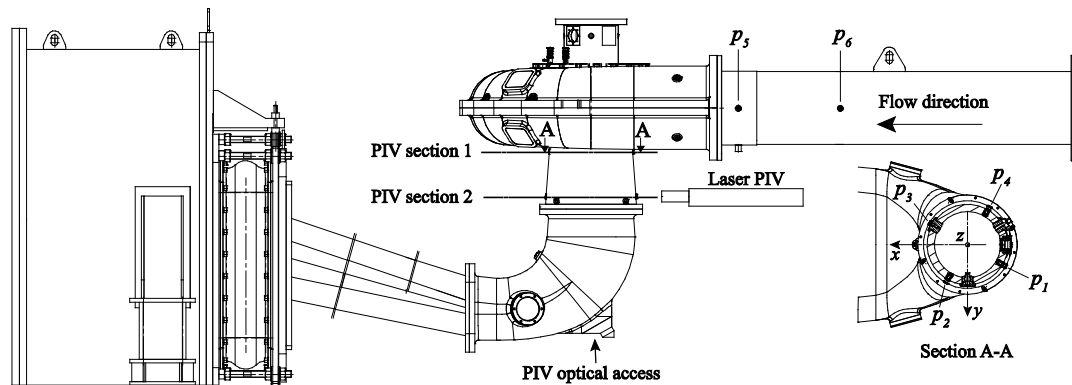


**Figure 1.** Reduced-scale physical model of a Francis turbine installed on EPFL test rig, together with the location of the pressure transducers and the PIV measurement sections.

## 3. Vortex dynamics in cavitation-free conditions

### 3.1. Flow regimes in cavitation-free conditions

Pressure measurements are first performed for a wide range of discharge factor values in cavitation-free conditions. The speed factor is kept constant at the rated value  $n_{ED} / n_{ED}^* = 1$ . The influence of the discharge on the precession frequency and the coherence between pressure signals measured in the cone is reported in Figure 2. Moreover, the corresponding auto-spectrum amplitude is given in Figure 3 for a pressure sensor located in the upstream pipe. This value can be directly linked to the intensity of the pressure excitation source as the measurements are taken in cavitation-free conditions and it is assumed there is no amplification of the synchronous pressure fluctuation as the first system eigenfrequency is sufficiently high.

Three flow regimes are highlighted depending on the value of the discharge factor [6]. The vortex rope starts developing within the first regime and is highly coherent and well-developed within the second regime, for which the precession frequency increases linearly as the discharge is decreased. At the same time, the excitation source intensity increases and reaches its maximum for a value of discharge equal to 65% of the rated value. Beyond 62% of the rated value (regime 3), the vortex rope loses its coherence and periodicity, which is illustrated in Figure 2-b by a drop in the value of  $C_{xy}$ . This results in a sudden decrease of the excitation source intensity, as shown in Figure 3.

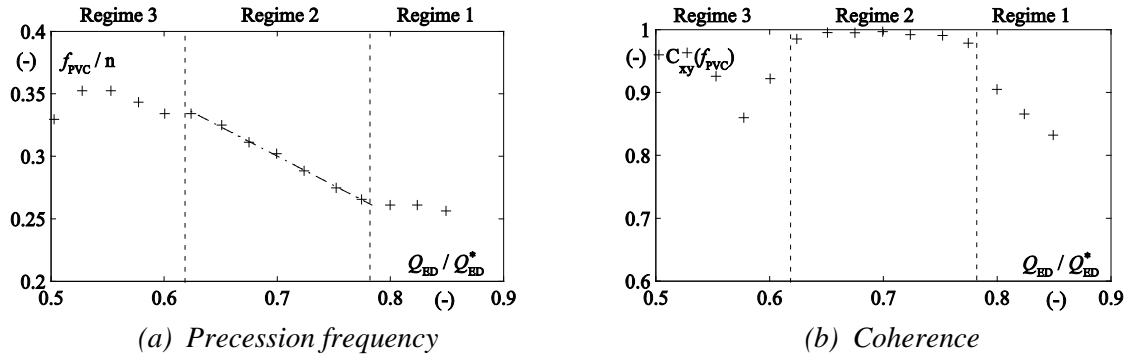


**Figure 2.** (a) Precession frequency made dimensionless by the runner frequency and (b) coherence at the precession frequency between pressure signals measured in the cone (sensors  $p_2$  and  $p_3$ ) as a function of the discharge factor –  $n_{ED}/n_{ED}^* = 1$ .

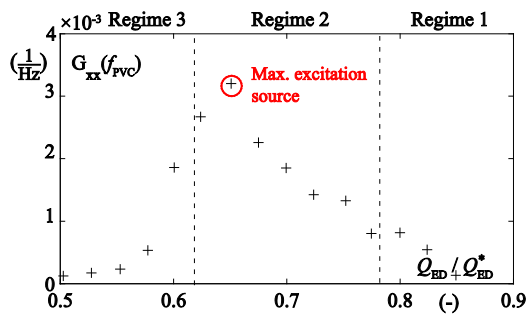


**Figure 3.** Influence of the discharge factor on the auto-spectrum amplitude at the precession frequency for pressure signals measured in the upstream pipe in cavitation-free conditions –  $n_{ED}/n_{ED}^* = 1$ .

### 3.2. Influence of the flow discharge on the vortex parameters

The tangential flow velocity fields are measured in two horizontal cross-sections of the cone by means of PIV performed in cavitation-free conditions for different values of the discharge factor to link the vortex parameters with the excitation source intensity. For each operating point, the vortex trajectory and circulation are determined by identifying the vortex centre and the vortex core limits with the algorithms proposed by Graftieaux et al. [8]. The influence of the discharge factor on both the vortex trajectory length and the vortex circulation is reported in Figure 4. When the discharge factor is decreased within the flow regimes 1 and 2, the vortex circulation increases while the vortex trajectory widens. They reach their maximum within the flow regime 2 for low discharge factor values when the excitation source intensity is also at its maximum. Beyond the transition from the regimes 2 to 3, the vortex trajectory slightly retracts and the determination of the vortex core limits and the computation of the vortex circulation are not possible anymore [6]. Based on these results, a physical mechanism responsible for the establishment of the pressure excitation source was proposed and discussed in [6]. The flow regime possibly leading to the highest pressure pulsations in case of resonance with the system would correspond to discharge factor values between 62 and 65% of the rated value.

## 4. Interaction with the system in cavitation conditions

### 4.1. Resonance conditions in cavitation conditions

In cavitation conditions, similar flow regimes are observed, as shown in Figure 5. The natural frequency is determined by cross-spectral analysis between two pressure signals measured in the cone [9]. Its value strongly decreases in the flow regime 1 when the discharge factor is decreased and is almost constant for low values of discharge factor in the flow regime 2. Resonance conditions occur for a discharge factor value equal to about 78% of the rated value for this  $n_{ED}$ -value. By varying the value of the speed factor, similar flow regimes and resonance conditions are observed with, however, a slight shift. This shift corresponds to that of the swirl-free conditions, see Figure 6-b.

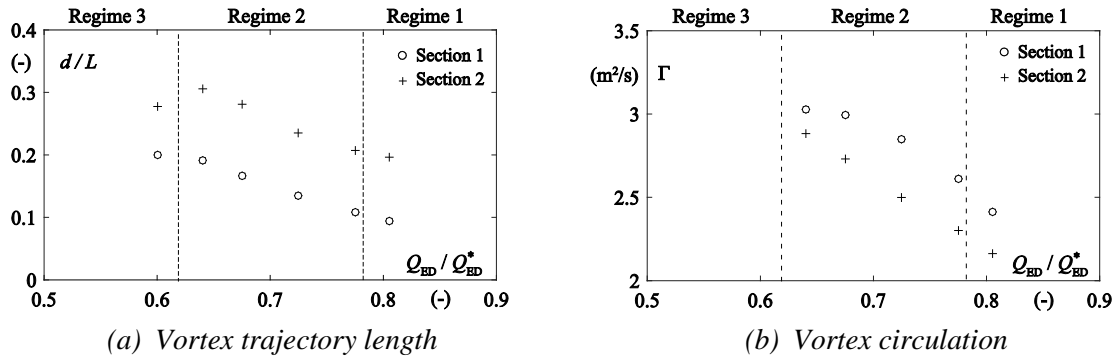


**Figure 4.** Influence of the discharge factor on the vortex trajectory and circulation in cavitation-free conditions –  $n_{ED} / n_{ED}^* = 1$ .

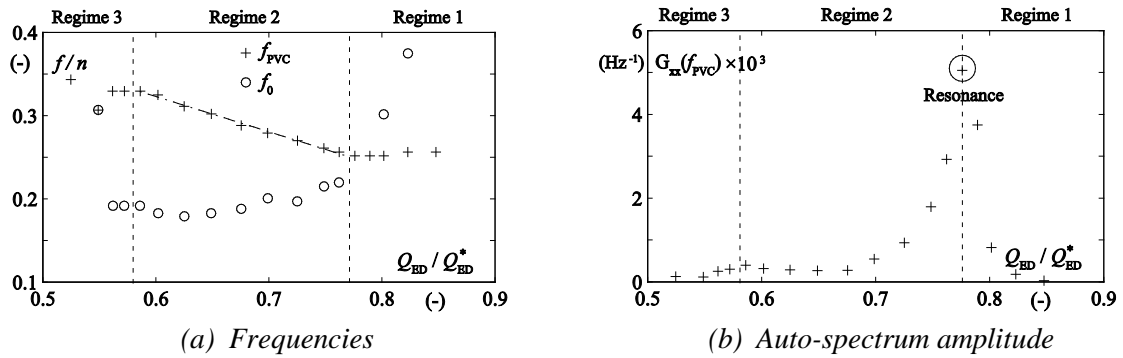


**Figure 5.** Influence of the discharge factor in cavitation conditions on the natural and precession frequencies and on the amplitude of the hydro-acoustic response of the system –  $n_{ED} / n_{ED}^* = 1$ .

#### 4.2. Resonance prediction at the model scale

The results described above show that the dynamics of the vortex and both precession and natural frequencies seem to be mainly driven by the degree of swirl of the flow. The latter can be characterized by the swirl number  $S$ , defined as the ratio between the axial flux of angular momentum and the axial flux of axial momentum. By assuming a constant axial velocity  $Cm = Q / \pi R^2$  and a solid-body rotation and by using the velocity triangles at the runner outlet, the swirl number can be expressed as a function of the speed and discharge factors:

$$S = n_{ED} \frac{\pi^2}{8} \left( \frac{1}{Q_{ED}} - \frac{1}{Q_{ED}^0} \right) \quad (1)$$

The Strouhal numbers  $St_{PVC} = f_{PVC} D^3 / Q$  and  $St_0 = f_0 D^3 / Q$  are plotted as a function of the swirl number in Figure 6-a by including all the investigated operating points. The data collapse in one linear function for the precession frequency and in one power function for the natural frequency. The swirl number for which resonances are expected to occur can be identified and is equal to  $S = 0.83$ . Based on this value, a relation between the speed and discharge factors in resonance conditions is derived:

$$Q_{ED}^{res} = 1 / \left( \frac{0.673}{n_{ED}} + \frac{1}{0.6674n_{ED} + 0.0516} \right) \quad (2)$$

In this expression, the value of the discharge factor  $Q_{ED}^0$  in swirl-free conditions is approximated by a linear fitting, see Figure 6-b. The occurrence of resonances can be finally predicted on the complete part load operating range by using Equation 2. The resonance conditions identified experimentally and the computed ones show an excellent agreement, see Figure 6-b. Further investigations will focus on the transposition of the natural frequencies to the prototype scale by using 1D SIMSEN models. Resonance

conditions will be finally predicted at the prototype scale and the results will be validated by on-site measurements performed on the prototype generating unit.

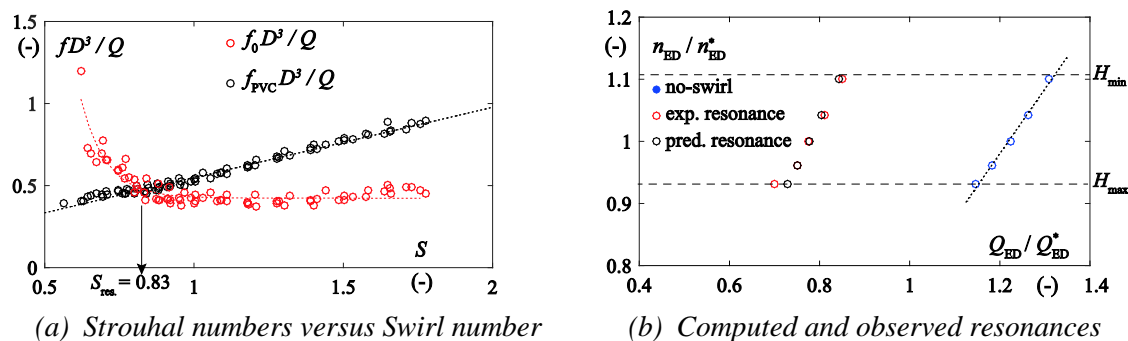


**Figure 6.** Strouhal numbers versus swirl number and comparison between computed and observed resonance conditions

## 5. Conclusion

Based on PIV survey coupled with pressure measurements, different flow regimes are highlighted, which depend on the value of the discharge. The link between the vortex dynamics and the pressure excitation source intensity is highlighted. The excitation intensity reaches its maximum when the flow circulation and the vortex trajectory are also at their maximum. Beyond a given value of discharge, the vortex dynamics lose its coherence and periodicity, resulting in a drop in the excitation intensity.

In cavitation conditions, similar flow regimes are observed and resonance conditions are identified by spectral analysis between pressure signals for different values of speed factor. It is shown that both precession and natural frequencies mainly depend on the degree of swirl of the flow exiting the runner. Empirical laws linking both precession and natural frequencies with the operating parameters are established, enabling the prediction of resonance conditions on the complete hillchart at the model scale.

These results demonstrate that the experimental determination of both precession and natural frequencies for a limited number of operating points enables finally the prediction of resonance conditions on the complete part load operating range. The results will be transposed to the prototype scale by using 1D SIMSEN model and the methodology will be validated by on-site measurements.

## Acknowledgements

The research leading to the results published in this paper is part of the HYPERBOLE research project, granted by the European Commission (ERC/FP7- ENERGY-2013-1-Grant 608532).

## References

- [1] Yamamoto K, Müller A, Favrel A, Landry, C and Avellan F 2015 *Proceedings of the 6<sup>th</sup> IAHR Workgroup, Ljubljana, Slovenia*
- [2] Müller A, Dreyer M, Andreini N and Avellan F 2013 *Experiments in Fluids* **54**
- [3] Nishi M, Matsunaga S, Kubota T and Senoo Y 1982 *Proceedings of the 10<sup>th</sup> IAHR Symposium, Tokyo, Japan*
- [4] Landry C, Favrel A, Müller A, Nicolet C and Avellan F 2016 *Journal of Hydraulic Research* **54** 185-196
- [5] Favrel A, Landry C, Müller A, Yamamoto K and Avellan F 2014 *IOP Conference Series: Earth and Environmental Science*
- [6] Favrel A, Müller A, Landry C, Yamamoto K and Avellan F 2015 *Experiments in Fluids* **56** 1-15
- [7] Favrel A 2016 *Dynamics of the cavitation precessing vortex rope for Francis turbines at part load operating conditions* EPFL Ph.D. Thesis, Lausanne
- [8] Graftieaux L, Michard M and Nathalie G 2001 *Measurement Science and Technology* **12** 1422-1429
- [9] Favrel A, Müller A, Landry C, Yamamoto K and Avellan F 2016 *Experiments in Fluids* **57** 168